Educational Administration: Theory and Practice
2024, 30(5) 14797-14809
ISSN: 2148-2403
https://kuey.net/

Research Article

Brain Cancer Growth Measurement By Length And Density Estimation Using Centroid Based Octal Axis Model

S. Prathiba[1*], B. Sivagami[2]

[1*]Research Scholar, Department of Computer Science & Research Centre, S.T. Hindu College, Nagercoil – 629002, Affiliated to Manonmaniam Sundaranar University, Abishekapatti, Tirunelveli – 627012, Tamil Nadu, India.
[2]Associate Professor, Department of Computer Science & Application, S.T. Hindu College, Nagercoil – 629002, Affiliated to Manonmaniam Sundaranar University, Abishekapatti, Tirunelveli – 627012, Tamil Nadu, India.

***Corresponding Author: S.** Prathiba
*Email: (prathibasuyambu26@gmail.com).

Citation: S. Prathiba, et al (2024), Brain Cancer Growth Measurement By Length And Density Estimation Using Centroid Based Octal Axis Model, *Educational Administration: Theory and Practice*, *30(5) 14797-14809*
Doi: 10.53555/kuey.v30i5.7441

ARTICLE INFO

ABSTRACT

Brain cancer growth measurement methods involve a combination of imaging techniques and computational analysis to accurately assess tumor size, volume, and progression. Traditional methods rely on manual measurements from MRI or CT scans, where radiologists outline the tumor boundaries to calculate changes in size over time. However, these manual approaches can be time-consuming and subject to variability. To enhance precision and efficiency, automated and semi-automated methods have been developed, utilizing advanced algorithms to quantify their growth. Brain cancer measurement is an important task in brain cancer diagnosis. It meets the challenges like less accuracy, unsupport for multi-direction based growth measurement, bounding box based center processing. Hence, this paper proposes a new cancer growth measure method namely 'Brain Cancer Growth Measurement by length and density estimation using Centroid based Octal Axis Model (BCGH-COAM)'. It works based on centroid based process and the octal directional axes. This method experimentally measures cancer region better than the existing methods.

1 INTRODUCTION

Brain cancer growth measurement is a critical aspect of diagnosing and monitoring the progression of brain cancer. Accurate assessment of cancer growth is essential for determining the stage of cancer, evaluating treatment efficacy, and planning surgical or therapeutic interventions. Advanced imaging techniques, such as MRI scans, provide detailed visualizations of brain cancer, enabling precise measurement of tumor size over time.

Segmentation techniques, both manual and automated, are employed to delineate the tumor boundaries and quantify its growth. Recent advancements in artificial intelligence and machine learning have further enhanced the accuracy and efficiency of these measurements, allowing for real-time analysis and more personalized treatment plans.

Konukoglu et al. (2010) proposed a parameter estimation method for reaction-diffusion tumor growth models using time series of medical images. This model calculates patient specific parameter of the model using the images of the patient taken at successive time instances. The inputs considered for this model are time series of Magnetic Resonance Images (MRI). The goodness of this method is that it showed itself to be a successful attempt for adapting the tumor growth models to patient images and creating "patient-specific" models. The pitfall of this method is that it fails to consider mass effect of the tumor in to account during parameter estimation methodology. Also, shrinkage of the tumor due to therapy or any other treatment is also not brought under consideration.

Chen et al. (2011) put forth a Finite Element Method (FEM) - based 3-D tumor growth and prediction system with the help of longitudinal kidney tumor images. Herein, the reaction-diffusion model is adopted to model the growth and spreading of tumor cells in the kidney. The goodness of this method is its feasibility

and efficiency. The pitfall of the method is that the mass effect of the tumor and the tissues surrounding the tumor area was not included for the consideration which demands furthermore sophisticated investigation.
Yoo et al. (2011) proposed a study which evaluates the natural growth rate of metastatic brain tumors in unique subset of patients with non-small cell lung cancer. Herein, the tumor volume was determined using V-works software (V.4.0) and T1 gadolinium enhanced MR images. The findings obtained from this study may help optimize patient management during follow-up. But using this study we cannot calculate the volumetric doubling time. Also the growth rate is calculated by considering metastatic brain tumor cells which comes under Stage – IV. Hence it shows differences while considering the tumors of various other stages.
Gomez-Roca et al. (2011) investigated the impact of the pre-treatment tumor growth rate (GR) on the evaluation of treatment response according to RECIST (Response Evaluation Criteria in Solid Tumors). This RECIST is the standard guideline for most clinical trials in oncology. This study achieves a better feasibility and usefulness of measuring the tumor growth rate during the pre-treatment. The drawback of this study is that the strategy loses its efficiency while considering larger series of medical images.
Kazmi et al. (2012) represented a hybrid CA (Cellular Automaton) model which integrates *insilico* models of solid tumor growth and the effect of bio reductive drug TPZ. Herein, used a decentralized computing paradigm called a CA (Cellular Automaton) which offers a flexible environment for carrying out sophisticated computations in several modalities. The goodness of this method is that it provides computerized model which discusses the behavior of bio-reductive drug inside solid tumor. The drawback of this model is its complexity and time consumption.
Papadogiorgaki et al. (2014) developed a new continuum model of Avascular glioma-tumor growth which can be adapted to real clinical scenarios. Herein, the input considered are the series of MRI slices from the patients with both low-grade and high-grade glioma, their initial diagnosis and the tumor growth rate at particular time interval. The positive side of this model is that, it is characterized by implantation simplicity and computational efficiency. At the same time, this is not superior to models with explicit details of networks and results accuracy which diminishes its quality.
Schiavina et al. (2014) had undergone a study to evaluate the relationships between patients clinical characteristics and growth pattern of Small Renal Masses (SRM). This study considered the database of 70 patients diagnosed with 72 SRMs within the period 1996 & 2013. Logistic regression models were used to calculate the predictive factors affecting the tumor growth kinetics. The long-term follow-up, through which better correlations between clinical predictors and tumor growth kinetics have been found. But the limitation of this study is due to its small number of patients database considered.
Yang et al. (2015) had undergone a study which reviewed a consecutive series of 21 patients with FNS (Facial Nerve Schwannomes) who had favorable – facial nerve function. This study reports the long-term follow-up and the factors affecting the growth of the tumor growth rate and initial tumor size are correlated together, which is valuable to direct clinical practice. The limitation of this study is that the case series is not large enough and in-order to achieve better accuracy larger samples are required.
Sallemi et al. (2015) presented an advanced and convivial algorithm for brain glioblastomas tumor growth modelization. In this model, the tumor growth is simulated based on Cellular Automata and Fast Marching method (CFMM). Herein, the inputs considered are twenty pathological MRI obtained from 3T MRI clinical scanner. This research holds its goodness by bridging the gap between advanced technologies and clinical practices. The pitfall of this model is that it fails to segment boundary and the curve of the tumor if the initial images is of poor quality, which in turn affects the tumor growth estimation.
Understanding the rate of tumor growth is vital for predicting patient outcomes and adjusting treatment strategies accordingly. Continuous monitoring and accurate measurement of brain cancer growth play a pivotal role in improving patient survival rates and quality of life. The existing growth measurement methods deliver the measurement only in horizontal and vertical directions. The pixel density oriented measurement is also calculated only in global model, and not in multi-zone model. The length oriented growth measurement is computed based on rectangle bounded region, which is an inaccurate approach, because tumor region grow in a circular model. These issues motivate this research to develop a new cancer growth measurement method namely 'Brain Cancer Growth Measurement by length and density estimation using Centroid based Octal Axis Model (BCGH-COAM)' to solve the aforementioned issues. This method measures the cancer region in both length wise and pixel-density wise using the axes based approach.

2 PROPOSED METHOD

Proposed method measures the cancer region based on centroid location and the eight directions oriented guided model. The key points of the proposed BCGH-COAM method are:

- Supports length wise growth measurement
- Supports pixel-density wise growth measurement
- Centroid based measuring model
- Measurement is done through the octal axis model
- Measurement progresses based on circular coverage path

- GUI based visual support by drawing circular coverage and octal directional axes
- Length based measurement result is converted from pixel-length to mille meter (mm).

The work flow diagram of the proposed BCGH-COAM method regarding the length based measurement is illustrated in Figure 1.

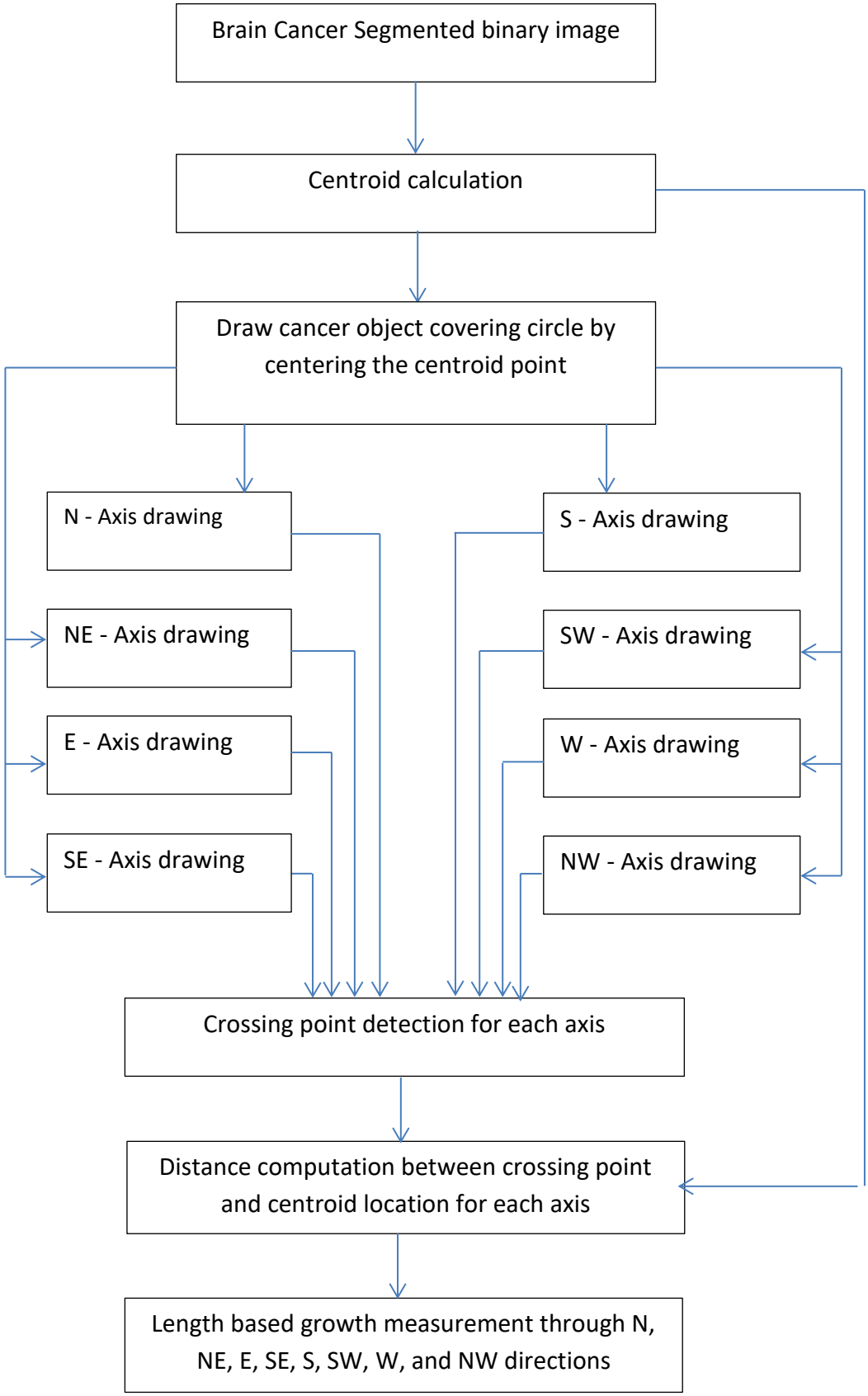

Fig.1: Block diagram for the length based growth estimation using the proposed BCGH-COAM method.

The proposed BCGH-COAM method accepts the cancer segmented output of the BCS-DDVNET method, as input. This input image is always be set in the binary form. The Figure 2(a) shows the input cancer object for illustration purpose.

Centroid is the centre point of the object that makes equidistant from its vertices. Imagine a frisbee and a person wants to make it spin on one finger. In order for it to spin, the exact center of the Frisbee must be located. The point that is in the exact center of a shape or object is known as the centroid. A circular shape like a frisbee has uniform density. When a shape has uniform density, the centroid is also the center of mass, which is the point at which the object will balance with just as much mass on all sides. This can also be called the center of gravity. When the centroid of the frisbee is located, it will make it possible for the frisbee to spin on one finger. Generally, cancer object in a MRI image has a partial circular shape in nature. Its growth is originated form its center location. But it is not an exact circle shape, hence, the center point of cancer object can be thought out as its centroid. This research plans to treat the centroid of the cancer object as its center point. The centroid can be spelled by other model, that the center point of the possibly smallest circle that covers the entire cancer/tumor is considered as its overall centroid location. According to Figure 1, the centroid of the input cancer object is found based on the following algorithm:

Step 1: Find the rectangle bounding box that covers the entire cancer region

Step 2: Find the center location of the bounding box

Step 3: Window size n=1

Step 4: Select n×n size window from the center bounding box center

Step 5: Find if there exist any locations in the window that can cover the entire cancer region in circular model. If there is such a pixel location then it is noted as the centroid location about that cancer object, otherwise, n=n+1, and repeat step 4 and step 5.

According to Figure 1, the possibly smallest circle that covers the entire cancer region is drawn over the cancer region. Figure 2(b) shows the circle that covers the entire cancer region.

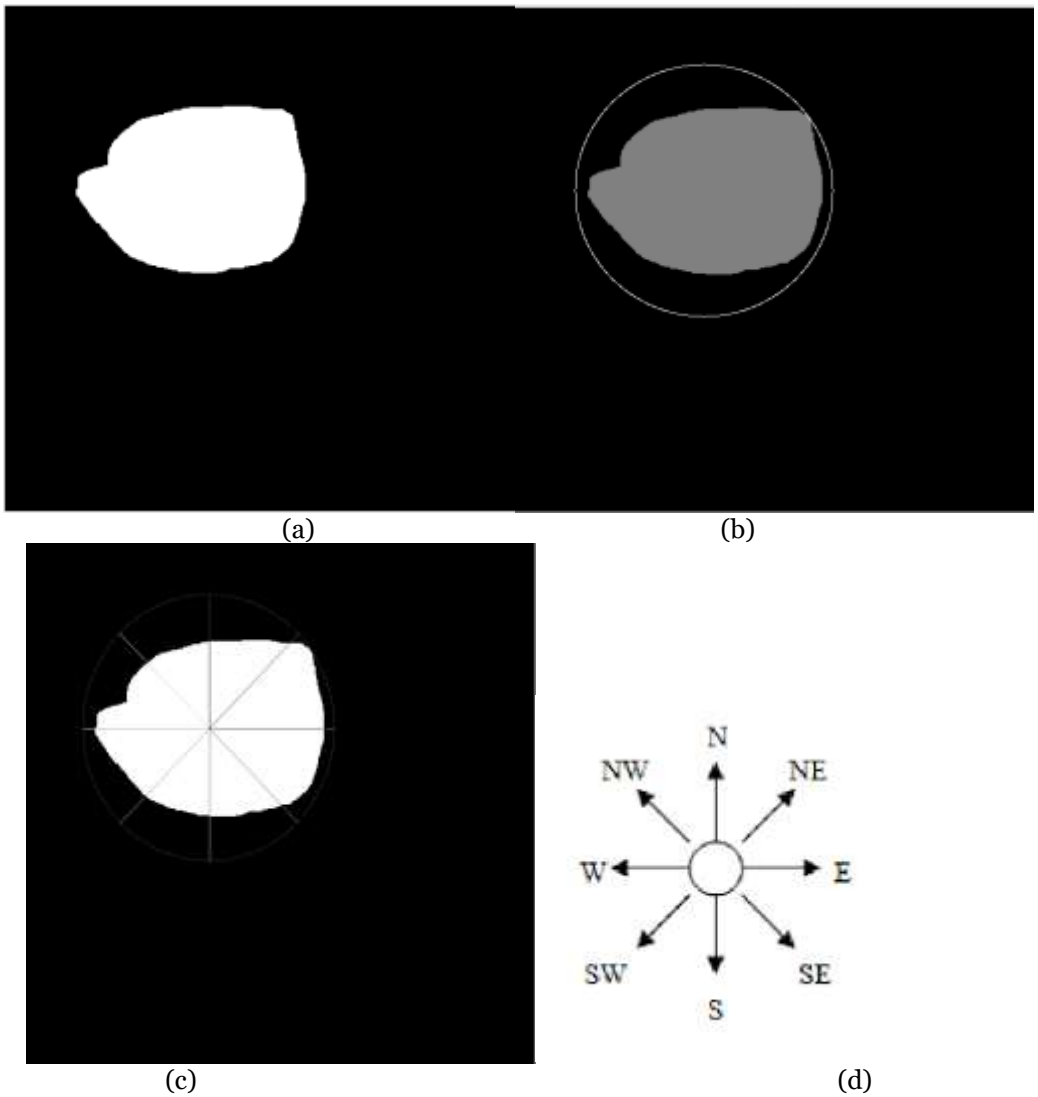

Fig. 5.2: Illustrating the model of the proposed BCGH-COAM method.

The eight axes that indicate the octal directions are drawn through the centroid location using the intensities 3 to 9. These various intensities ensure the differentiation in each axis. The intensity 0 is used to indicate the background, 1 is used to indicate the cancer object, and 2 is used to indicate the circle. This octal axis pattern is shown in Figure 2(c). These axes are named based on Figure 2(d). The crossing point (i.e., (x1,y1)) between the North axis, i.e., N-axis and the contour of cancer is found, and the distance between that crossing location and the centroid location (i.e., (x,y)) is found using Equation (1).

$$N_{DIST} = \sqrt{(x1 - x)^2 + (y1 - y)^2} \quad (1)$$

where

N_{DIST} - Length of growth measure in pixels in North direction

The crossing point (i.e., (x2,y2)) between the North-East axis, i.e., NE-axis and the contour of cancer is found, and the distance between that crossing location and the centroid location (i.e., (x,y)) is found using Equation (2).

$$NE_{DIST} = \sqrt{(x2 - x)^2 + (y2 - y)^2} \quad (2)$$

where

NE_{DIST} - Length of growth measure in pixels in North-East direction

In the similar model, the other distances corresponding to E, SE, S, SW, W, and NW directions are computed.

Generally, a single pixel is equal to the length of 0.2646 mm; hence, the actual length for the North direction is computed using Equation (3).

$$N_{DIST} = N_{DIST} \times 0.2646 \quad (3)$$

In the similar model, the cancer growth length corresponding to the other directions are also computed using Equation (3).

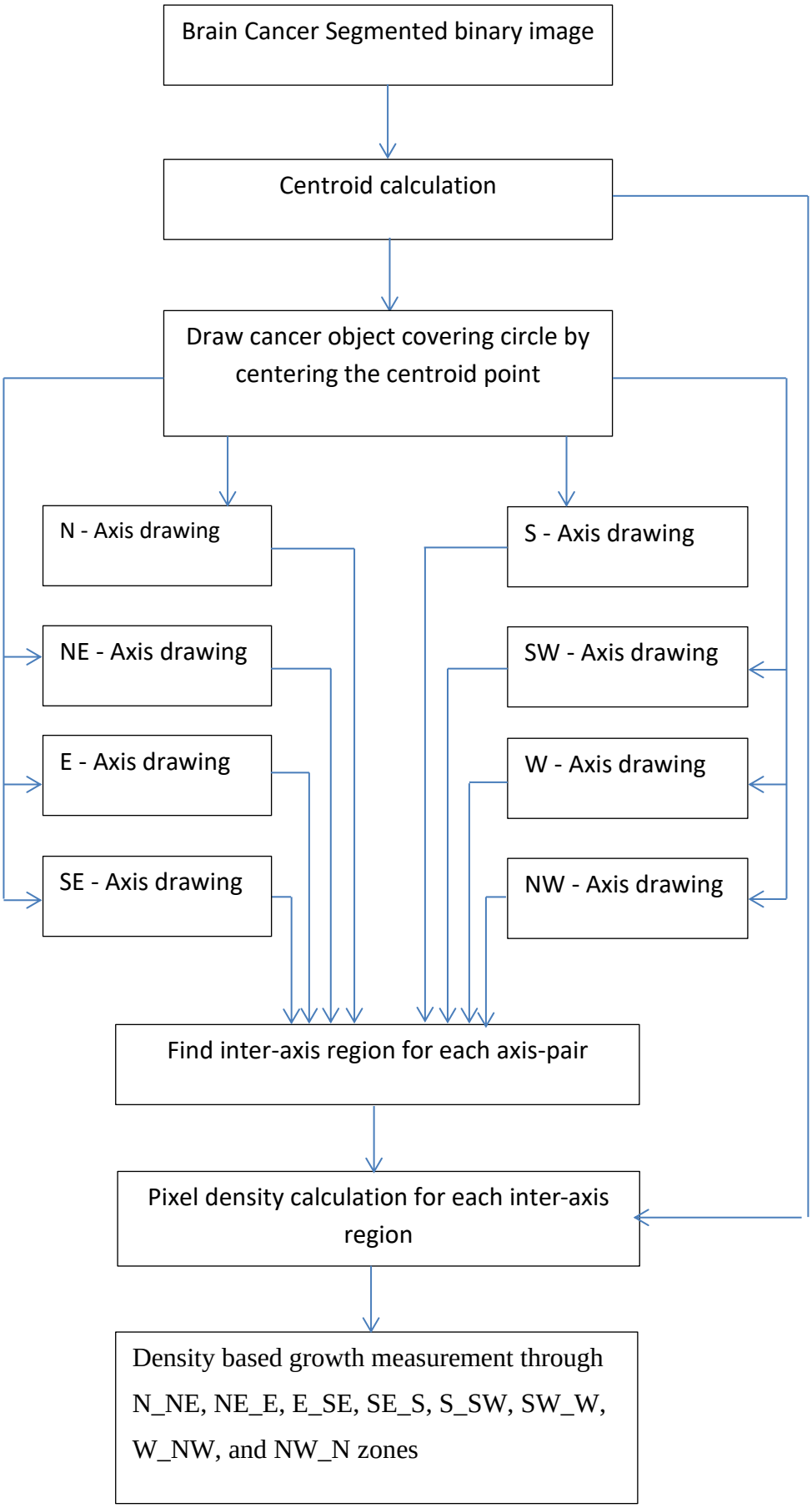

Fig.3 Block diagram for the density based growth estimation using the proposed BCGH-COAM method.

Pixel density based growth measurement means the count of pixels involved in the cancer region. The Global pixel density based growth measurement means the count of pixels in the entire cancer region irrespective to the axis path. In this research, a new growth measurement scheme is proposed for reporting the growth measurement based on pixel density (or simply density) using the centroid and octal axes. The proposed BCGH-COAM method reports the growth measurement regarding the eight zones such as N-NE, NE-E, E-SE, SE-S, S-SW, SW-W, W-NW, and NW-N. The entire process is described in Figure 3. The algorithm used to compute the proposed density based measurement is given below:

Step 1: Input the brain cancer segmented image
Step 2: Find the centroid location
Step 3: Draw covering circle based on centroid
Step 4: Draw axes regarding N, NE, E, SE, S, SW, W, and NW directions
Step 5: Find Pixel density for the N-NE zone
Step 6: Find Pixel density for the NE-E zone
Step 7: Find Pixel density for the E-SE zone
Step 8: Find Pixel density for the S_ES zone
Step 9: Find Pixel density for the S-SW zone
Step 10: Find Pixel density for the SW-W zone
Step 11: Find Pixel density for the W-NW zone
Step 12: Find Pixel density for the NW-N zone.

The eight different zones can be understood using Figure 2(c) and Figure 2(d). The eight density based growth measurements are delivered as report to the oncologists.

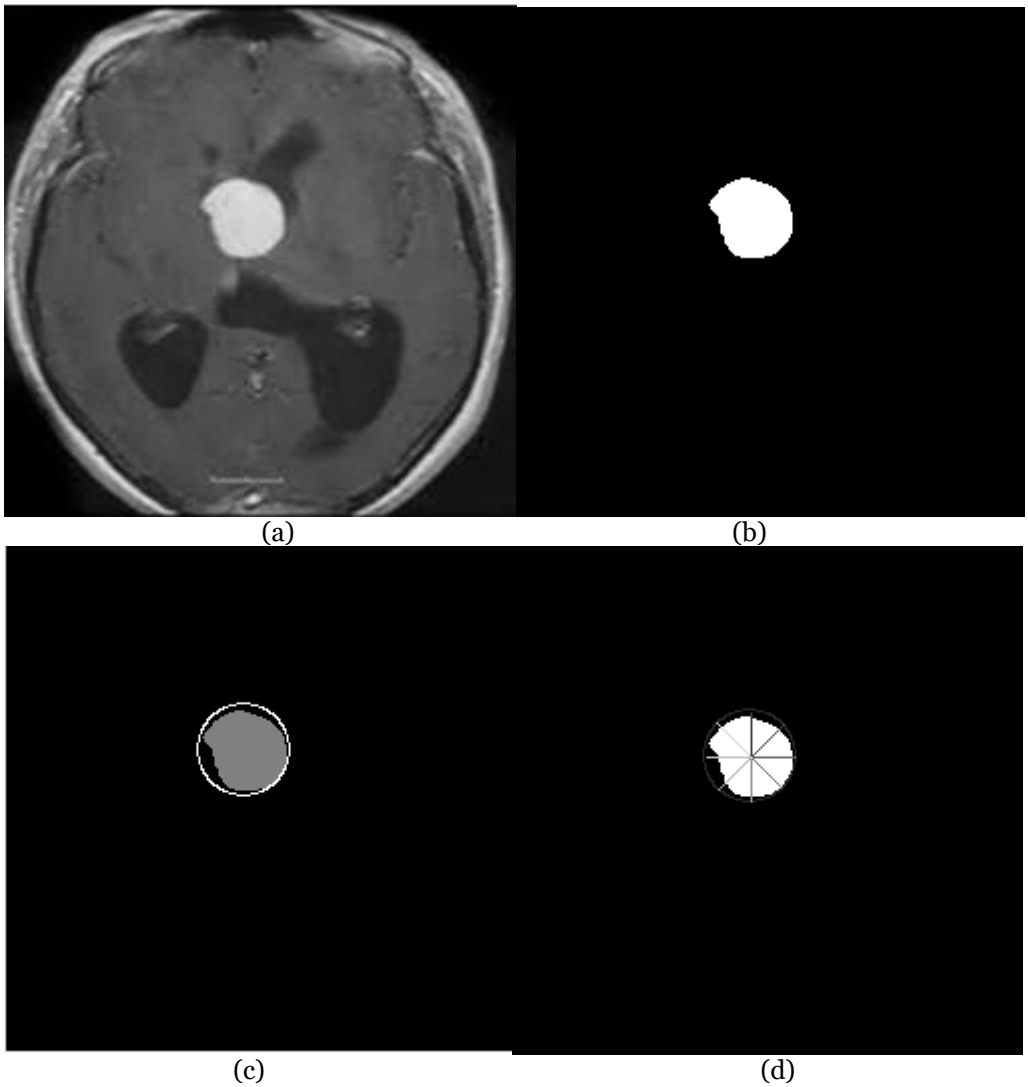

(a) (b)

(c) (d)

N Direction Tumor growth= 5.027 mm

NE Direction Tumor growth= 4.864 mm

E Direction Tumor growth= 5.292 mm

SE Direction Tumor growth= 5.238 mm

S Direction Tumor growth= 5.027 mm

SW Direction Tumor growth= 4.490 mm

W Direction Tumor growth= 4.233 mm

NW Direction Tumor growth= 5.613 mm

(e)

Zone N-NE density= 150

Zone NE-E Density= 159

Zone E-SE Density= 175

Zone SE-S Density= 160

Zone S-SW Density= 154

Zone SW-W Density= 111

Zone W-NW Density= 174

Zone NW-N Density= 170

(f)

Fig.4 Sample screen for the proposed growth measure method BCGH-COAM for Sample-image-1; (a) noise-free image, (b) cancer segmented image, (c) centroid based circular coverage, (d) Octal axes representation, (e) length based growth report, (f) density based growth report.

Figure 4 shows the outputs of the BCGH-COAM method for Sample-image-1. Figure 4(a) shows the noise-free MRI image that is delivered by the proposed IHSMW filter. Figure 4(b) shows the cancer segmented image delivered by the proposed BCS-DDVNET method. Figure 4(c) shows the coverage circle of cancer region, and Figure 4(d) shows the octal axes model. Figure 4(e) shows the length based growth measurement report, and Figure 4(f) shows the density based growth measurement report.

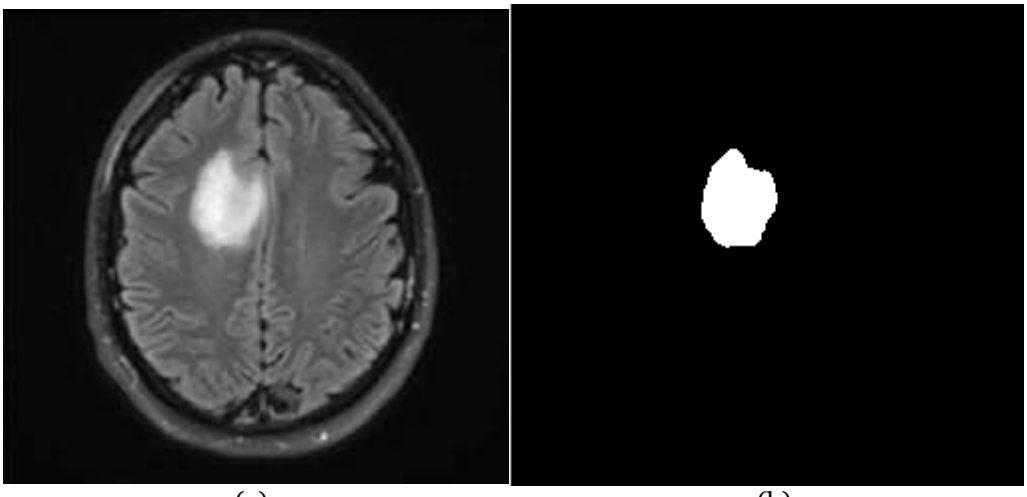

(a)

(b)

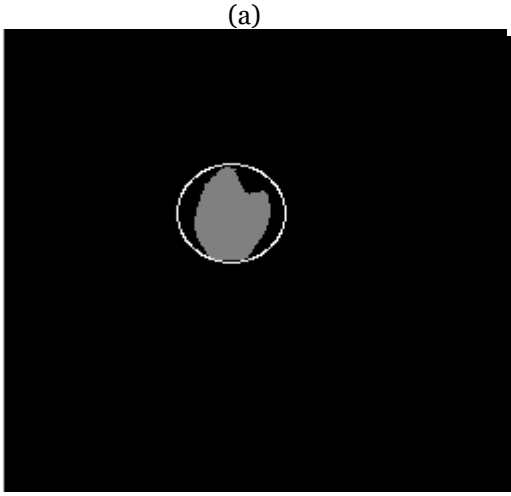

(c)

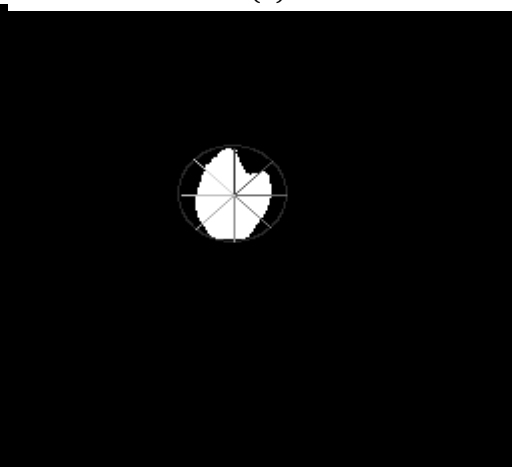

(d)

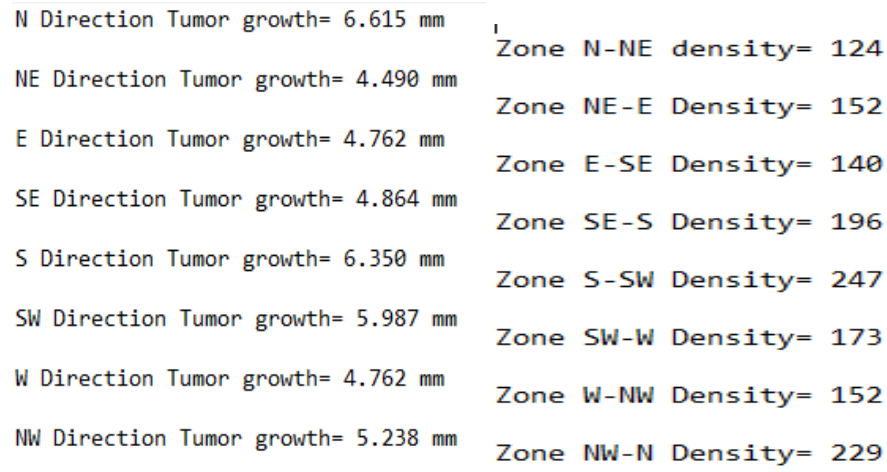

Fig.5: Sample screen for the proposed growth measure method BCGH-COAM for Sample-Image-2; (a) noise-free image, (b) cancer segmented image, (c) centroid based circular coverage, (d) Octal axes representation, (e) length based growth report, (f) density based growth report.

Figure 5 depicts the outputs of the BCGH-COAM method for Sample-image-2 image. Figure 5(a) shows the noise-free MRI image and Figure 5(b) shows the cancer segmented image. Figure 5(c) depicts the coverage circle of cancer region, and Figure 5(d) shows the octal axes pattern. Figure 5(e) shows the length based growth measurement report, while Figure 5(f) shows the density based growth measurement report.

5.3. DISCUSSION AND ANALYSIS

The length based measurement through the proposed BCGH-COAM method is applied for the three existing cancer segmentation methods such as BCS-SRN (Ding et al. 2019), BCS-GED (Gawad et al. 2020), and BCS-HSCRD(Ejaz et al. 2021), and BCS-DDVNET (Prathiba et al. 2024). The growth error rate is computed regarding the length based measurement through the BCGH-COAM method. First, the ground-truth cancer object segmentation is prepared for a specific MRI image, and the resultant output undergoes the length based measurement through the BCGH-COAM method. Second, the automatic cancer segmentation for the same image derived, and the resultant output undergoes the length based measurement through the BCGH-COAM method. The absolute difference between the 'ground-truth oriented data' and the 'automatic segmentation oriented data' is noted as the growth estimation error. This process is done for the eight axes oriented data. This scheme can be illustrated using the range of equations from Equation (4) to Equation (11).

$$N_{GErr} = |N_{Gnd} - N_{Seg}| \quad (4)$$

$$NE_{GErr} = |NE_{Gnd} - NE_{Seg}| \quad (5)$$

$$E_{GErr} = |E_{Gnd} - E_{Seg}| \quad (6)$$

$$SE_{GErr} = |SE_{Gnd} - SE_{Seg}| \quad (7)$$

$$S_{GErr} = |S_{Gnd} - S_{Seg}| \quad (8)$$

$$SW_{GErr} = |SW_{Gnd} - SW_{Seg}| \quad (9)$$

$$W_{GErr} = |W_{Gnd} - W_{Seg}| \quad (10)$$

$$NW_{GErr} = |NW_{Gnd} - NW_{Seg}| \quad (11)$$

where

N_{GErr} - North direction growth error
NE_{GErr} - North-East direction growth error
E_{GErr} - East direction growth error
SE_{GErr} - South-East direction growth error
S_{GErr} - South direction growth error
SW_{GErr} - South-West direction growth error
W_{GErr} - West direction growth error
NW_{GErr} - North-West direction growth error

Table 1: Cancer growth error analysis based on length oriented measurement

Method	Cancer growth error							
	NE	SW	W	E	N	S	NW	SE
BCS-SRN	0.604	0.638	0.654	0.628	0.683	0.641	0.605	0.639
BCS-GED	0.584	0.545	0.529	0.522	0.530	0.510	0.518	0.525
BCS-HSCRD	0.426	0.404	0.398	0.428	0.437	0.410	0.425	0.438
BCS-DDVNET	0.251	0.310	0.263	0.205	0.320	0.288	0.342	0.232

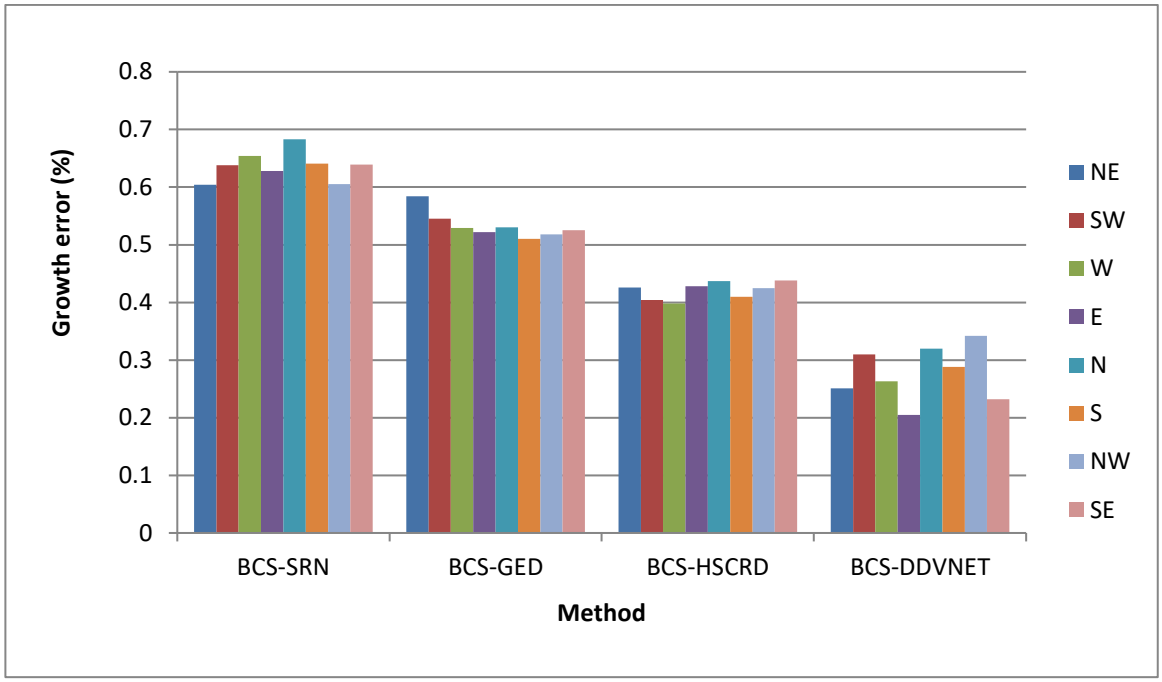

Fig.6: Cancer growth error analysis chart.

Table 1 and Figure 6 show the cancer growth error analysis based on the length based approach of the proposed BCGH-COAM method. This analysis is carried out based on 100 test images that are randomly selected from the four datasets, through the averaging process. This analysis proves that the BCS-DDVNET method reaches the less growth error level in the entire eight directions than the existing methods; hence, it is called the best segmentation method. The BCS-HSCRD method is known as second-best method, since it reaches secondary level errors. The BCS-SRN method is the least performer in cancer segmentation because it occupies higher error levels.

The cancer growth error rate is computed using density based measurement of the proposed BCGH-COAM method. The ground-truth based North direction measurement is computed and stored as N_{Gnd}. The segmentation output based North direction measurement is computed and stored as N_{Seg}. The North direction cancer growth error rate N_{GErr} in percentage is computed using Equation (12).

$$N_{GErr} = \frac{100}{N_{Gnd}} \times N_{Seg} \quad (12)$$

In the similar model, the other direction measurements are also computed.

Table 2: Cancer growth error analysis based on density oriented measurement

Method	Cancer growth error (in %)							
	NE	SW	W	E	N	S	NW	SE
BCS-SRN	1.62	1.60	1.59	1.45	1.67	1.71	1.53	1.57
BCS-GED	1.41	1.52	1.33	1.28	1.57	1.69	1.66	1.52
BCS-HSCRD	1.16	1.22	1.23	1.18	1.40	1.61	1.58	1.29
BCS-DDVNET	0.67	0.74	0.83	0.65	0.70	0.56	0.61	0.53

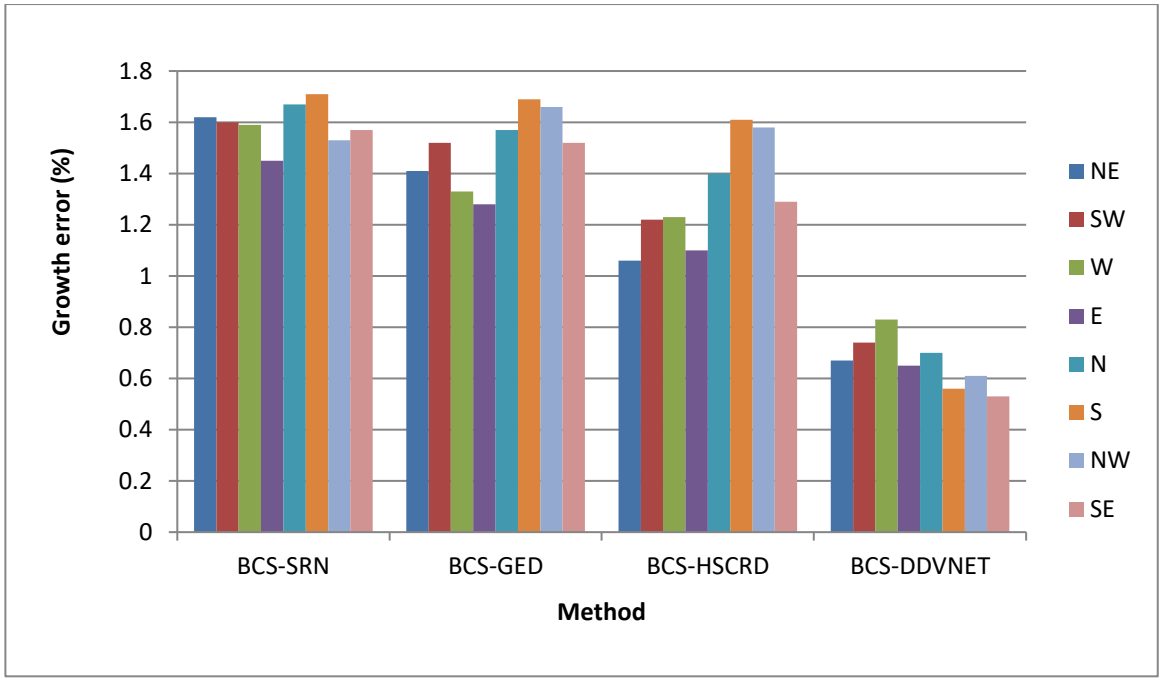

Fig.7: Density based cancer growth error rate analysis chart.

Table 2 and Figure 6 show the density based growth error rate analysis regarding the proposed BCGH-COAM method. The less error produced method is called best segmentation method. The BCS-DDVNET method generates less error percentage than the existing methods. The least error produced by the BCS-DDVNET method is 0.53%. The highest error produced by the BCS-DDVNET method is 0.83%. Hence, it is called the best cancer segmentation method. The BCS-HSCRD method reaches the range of errors from 1.16% to 1.61%. Hence, it is called the second-best method for cancer segmentation. The BCS-GED method is noted as the third-best method, while the BCS-SRN method is noted as the least performer due to its highest error rates.

Table 3: Global density based cancer growth error analysis

Method	Cancer growth error (in %)
BCS-SRN	12.74
BCS-GED	11.98
BCS-HSCRD	10.41
BCS-DDVNET	5.29

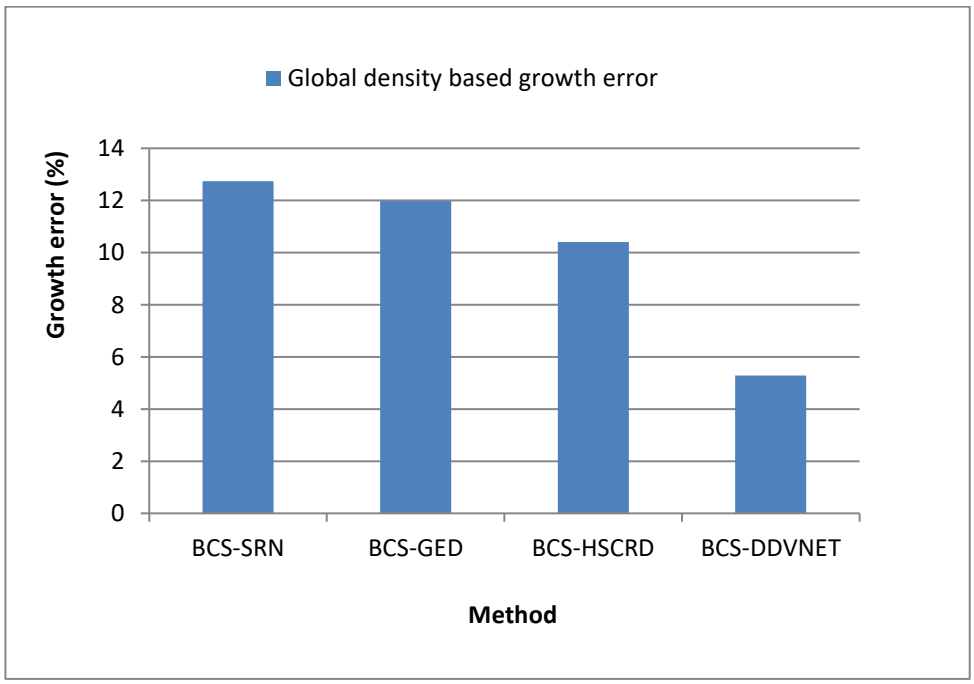

Fig.8: Global Density based cancer growth error rate analysis chart.

Table 3 and Figure 8 show the global density based cancer growth error rate analysis for the four methods. This analysis proves the minimum range error level (i.e., 5.29%) of the BCS-DDVNET segmentation method. It also reveals the highest error level of the BCS-SRN method. This analysis proves that the BCS-DDVNET method is the best cancer segmentation method than the existing methods.

Table 4: Characteristics of the existing and proposed cancer measurement methods

Growth measurement method	**characteristics**
Global density	Gives only the pixel count in the entire cancer region. Does not yield direction based density info
Horizontal/vertical length method	Gives either horizontal direction length or the vertical direction length Does not yield multi direction based length info Gives pixels based measurement not mille meter based model
Four axis based model	Gives only four directions based cancer length Does not yield eight directions based cancer length Does not yield eight directions based cancer density info Less accurate cancer growth measurement due to the rectangle bounding box based process
Proposed BCGH-COAM	Gives octal directions based cancer length Gives octal directions based cancer growth by density info More accurate cancer measurement due to the centroid based process Length measurement is provided in mille meter unit which is more practical

Table 4 shows the specific characteristics of the existing and the proposed cancer measurement methods. This table shows the pros and cons of the cancer growth measurement methods. From this table it is proved that the proposed BCGH-COAM method much better than the existing methods.

4 Conclusion

The proposed BCGH-COAM method successfully measures the cancer growth based on centroid and octal axis based approaches. This method is applied for the four cancer segmentation methods such as BCS-SRN, BCS-GED, BCS-HSCRD, and the BCS-DDVNET to measure the cancer growth. The proposed BCGH-COAM method delivers less growth error for the BCS-DDVNET method using both length and density based models. The pros of the proposed BCGH-COAM method are (i) octal directions based cancer length, (ii) octal directions based cancer growth by density info, (iii) centroid based process, and (iv) mm based length measurement.

Reference

1. Ding Y., Chen F., Zhao Y., Wu Z., ZhangC.and Wu D., 2019, 'A Stacked Multi-Connection Simple Reducing Net for Brain Tumor Segmentation' *IEEE Access*, vol. 07, pp. 104011-104024.
2. Gawad A.H.A., Said A.L. and Radwan A.G., 2020, 'Optimized Edge Detection Technique for Brain Tumor Detection in MR Images', *IEEE Access*, vol. 08, pp. 136243-136259.
3. Ejaz K., Rahim M.S.M.,Bajwa U.I.,Chaudhry H.,Rehman A. and Ejaz F., 2021,'Hybrid Segmentation Method With Confidence Region Detection for Tumor Identification', *IEEE Access*, vol. 09, pp. 35256-35278.
4. S. Prathiba and Dr. B. Sivagami, 2024 "Bts-Vnet: Brain Tumour Segmentation Via Deep Learning Based Dual Attention Integrated V-Network", O & G Forum, Issue 3, pp. 2943 -2951.
5. Yang W., Zhao J., Han Y., Yang H., Xing J., Zhang Y., Wang Y., and Liu H., 2015, 'Long-term outcomes of facial nerve schwannomas with favorable facial nerve function: tumor growth rate is correlated with initial tumor size', Elsevier, Science Direct, vol. 36, issue 2, pp. 163-165.
6. Papadogiorgaki M., Kounelakis M.G., Koliou P., and Zervakis M.E., 2015, 'A Glycolysis-Based In Silico Model for the Solid Tumor Growth', *IEEE journal of biomedical and health informatics*, vol. 19, issue 3, pp. 1106-1117.
7. Kazmi N., Hossain M.A., and Phillips R.M., 2012, 'A Hybrid Cellular Automaton Model of Solid Tumor Growth and Bioreductive Drug Transport' *IEEE/ACM transactions on computational biology and bioinformatics*, vol. 9, issue 6, pp. 1595-1606.
8. Gomez-Roca C., Koscielny S., Ribrag V., Dromain C., Marzouk I., Bidault F., Bahleda R., Ferté C., Massard C., Soria J.C., 2011, 'Tumour growth rates and RECIST criteria in early drug development', Elsevier, European journal of cancer, vol. 47, issue 17, pp. 2512-2516.

9. Yoo H., Jung E., Nam B. H., Shin S.H., Gwak H.S., Kim M.S., Zo J.I., Lee S.H., 2011, 'Growth rate of newly developed metastatic brain tumors after thoracotomy in patients with non-small cell lung cancer', Elsevier, Lung Cancer, vol. 71, issue 2, pp. 205-208. Konukoglu E. *et al.,* 2010, 'Image Guided Personalization of Reaction-Diffusion Type Tumor Growth Models Using Modified Anisotropic Eikonal Equations', *IEEE transactions on medical imaging,* vol. 29, issue 1, pp. 77-95.
10. Chen X., Summers R., and Yao J., 2011, 'FEM-Based 3-D Tumor Growth Prediction for Kidney Tumor', *IEEE transactions on biomedical engineering*, vol. 58, issue 3, pp. 463-467.
11. Schiavina R., Borghesi M., Dababneh H., Bianchi L., Longhi B., Diazzi D., Monti C., Manna G.L., Martorana G., and Brunocilla E., 2014, 'Small Renal Masses Managed With Active Surveillance: Predictors of Tumor Growth Rate After Long-Term Follow-Up', Elsevier, vol. 13, issue 2, pp. 87-92.
12. Sallemi L., Njeh I., and Lehericy S., 2015, 'Towards a Computer Aided Prognosis for Brain Glioblastomas Tumor Growth Estimation', *IEEE Transactions on nanobioscience,* vol. 14, issue 7, pp. 727-733.